

## Modeling of the mechanism of reductive allylation of norbornadiene in the presence of Pd<sup>0</sup> complexes

R. S. Shamsiev,\* K. T. Egiazaryan, and V. R. Flid

MIREA — Russian Technological University, M. V. Lomonosov Institute of Fine Chemical Technologies, 86 prosp. Vernadskogo, 119571 Moscow, Russian Federation.  
Fax: +7 (495) 434 9287. E-mail: Shamsiev.R@gmail.com

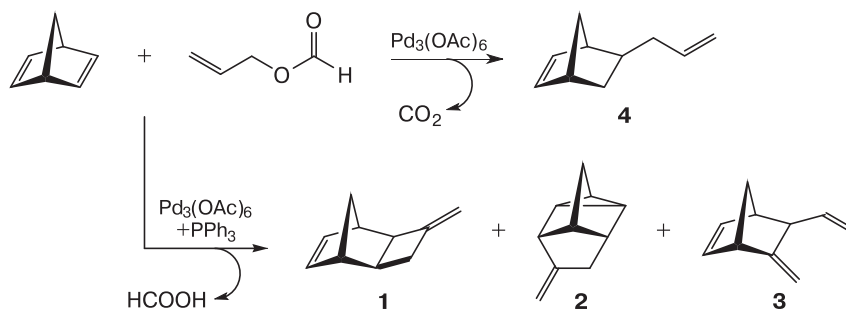
Hydroallylation of norbornadiene (NBD) with allyl formate (AF) in the presence of the Pd<sup>0</sup> complexes with the formation of 5-allyl-2-norbornene was modeled by the method based on the DFT-PBE/L11 density functional theory. According to the calculation results, 5-allyl-2-norbornene is formed *via* two mechanisms. The first assumes that the C–C bond between the NBD and allyl ligand is formed before the cleavage of the formyl C–H bond and elimination of CO<sub>2</sub>, whereas following the second mechanism the bond is formed after these processes. For both mechanisms, Pd(AF)(MeCN) is the catalytically active complex and C<sub>NBD</sub>–C<sub>All</sub> bond formation is the rate-determining step with the Gibbs activation energy equal to 22.8 and 21.3 kcal mol<sup>–1</sup> for the first and second mechanisms, respectively. High selectivity to 5-allyl-2-norbornene in the absence of phosphine ligands is attributable to the kinetically hindered formation of the second C–C bond needed for the generation of product of oxidative allylation of NBD. The predominance of the *exo*-substituted product is due to the formation of the thermodynamically stable complex with the bidentate coordination of NBD favored by the *endo*-coordination of the NBD molecule.

**Key words:** norbornadiene, allylation, palladium, allyl formate, reaction mechanism, density functional theory.

The catalytic reactions of bicyclo[2.2.1]hepta-2,5-diene (norbornadiene, NBD) with allyl carboxylates afford various norbornene derivatives containing two or more double bonds with diverse reactivities.<sup>1–7</sup> The Ni<sup>0</sup> complexes stabilized by phosphite ligands are most active in the catalytic allylation of norbornene and NBD.<sup>2–6</sup> The palladium catalysts<sup>7–9</sup> are less active and selective, but the use of palladium acetate Pd<sub>3</sub>(OAc)<sub>6</sub> as the catalyst precursor makes it possible to involve in the reaction a new allylating agent, allyl formate (AF). This cannot be achieved in the Ni-catalyzed allylation of NBD because of the high sensitivity of the catalytic system to oxygen.

The major products of the oxidative allylation of NBD, *viz.*, 3-methylenetricyclo[4.2.1.0<sup>2,5</sup>]non-7-ene (**1**), 8-methylenetricyclo[4.3.0.0<sup>2,4</sup>.0<sup>3,7</sup>]nonane (**2**), and 5-methylene-6-vinylbicyclo[2.2.1]hept-2-ene (**3**), as well as the reductive allylation product 5-allyl-2-norbornene (**4**), are presented in Scheme 1. The structures of the products indicate that the allyl fragment can be incorporated into the NBD molecule *via* different routes: with retention of the allyl fragment (products **1**, **2**, and **4**) or with the cleavage of the C–C allyl bond (**3**). Since during reductive allylation the NBD molecule withdraws the allyl group and H atom from the AF molecule, structure **4** can be

Scheme 1



considered to be the product of NBD hydroallylation. Reductive allylation is not characteristic of the Ni-catalyzed allylation of NBD, and product **4** is not formed in the presence of the Ni complexes.

Based on the literature data,<sup>8,9</sup> we may conclude that the mechanism of reductive allylation of NBD in the presence of the Pd<sub>3</sub>(OAc)<sub>6</sub>/AF/NBD/MeCN system includes the following steps: oxidative addition of AF to form the palladium η<sup>3</sup>-allyl complex, η<sup>3</sup>–η<sup>1</sup>-isomerization of the allyl ligand, formation of C–C bonds, and hydride transfers. In the induction (initial) period, the Pd<sup>II</sup> acetate complex is reduced to Pd<sup>0</sup> acetonitrile complexes. The hydride transfer from the formyl ligand to palladium occurs (with a high probability) in the course of the rate-determining step, which is indicated by the kinetic isotope effect (KIE = 2.2) in NBD hydroallylation.<sup>8,9</sup>

Another distinction of the palladium system from the nickel one is that the Pd/PPh<sub>3</sub> molar ratio weakly affects the reaction selectivity. At the same time, in the absence of phosphine ligands, the reaction affords product **4** with high selectivity<sup>6</sup> (up to 90–95%). To optimize the conditions for the formation of individual products with the highest selectivity, a knowledge of the detailed mechanism of the process of catalytic allylation is needed. Therefore, quantum chemical modeling of the mechanism for the formation of the product of NBD hydroallylation in the presence of the Pd<sup>0</sup> acetonitrile complexes is of significant interest.

### Calculation Methods

Calculations were performed using the PRIRODA program (see Refs 10 and 11) in the framework of the all-electron scalar relativistic approach of the density functional theory (DFT). The PBE exchange correlation functional<sup>12</sup> combined with the L11 basis set<sup>13</sup> was used with the following scheme of orbital contraction: Pd (26s23p16d5f)/[7s6p4d1f], O and C (10s7p3d)/[4s3p1d], and H (6s2p)/[2s1p]. This procedure has previously been applied<sup>14,15</sup> to study the mechanisms of the catalytic reactions involving NBD.

The correspondence of the optimized structures to minima or to transition states (TS) was confirmed by frequency analysis.

The internal reaction coordinate (IRC) was calculated to check the evolution relationship of the found TS to the minima. The thermodynamic parameters ( $\Delta G_{298}$ ,  $\Delta G_{298}^\ddagger$ ) were calculated at  $T = 298$  K. A correction to the solvation energy (solvent acetonitrile,  $\epsilon = 38$ ) was estimated in the framework of the IPCM polarizable continuum model (Isodensity PCM).

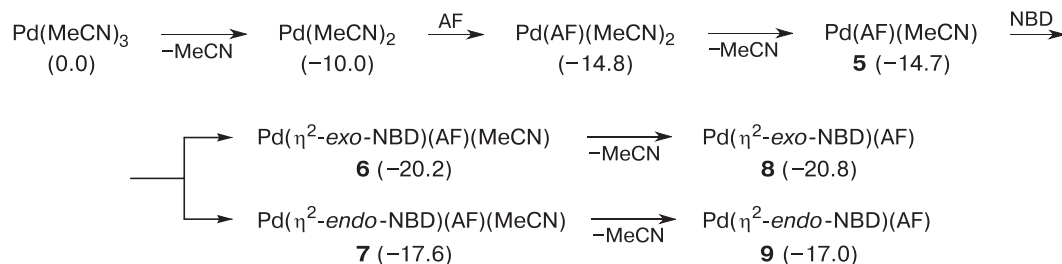
### Results and Discussion

The thermodynamic characteristics of mutual transformations between the Pd<sup>0</sup> complexes in the presence of AF, NBD, and MeCN as the solvent are presented in Scheme 2. The Pd(MeCN)<sub>3</sub> complex was considered as the initial complex in modeling.

The consecutive displacement of the acetonitrile ligand and coordination of the AF molecule with the formation of complexes Pd(AF)(MeCN)<sub>2</sub> and Pd(AF)(MeCN) (**5**) are energetically favorable. It is known<sup>14,15</sup> that two η<sup>2</sup> modes are possible for the coordination of the NBD molecule: with the formation of Pd(η<sup>2</sup>-*exo*-NBD)(AF)(MeCN) (**6**) and Pd(η<sup>2</sup>-*endo*-NBD)(AF)(MeCN) (**7**). *exo*-Coordination of NBD is by 2.6 kcal mol<sup>-1</sup> more advantageous than *endo*-coordination. The further elimination of the acetonitrile ligand to form Pd(η<sup>2</sup>-*exo*-NBD)(AF) (**8**) is thermodynamically favorable (by 0.6 kcal mol<sup>-1</sup>) for complex **6**. In the case of complex **7**, the elimination of the acetonitrile ligands gives a 0.6 kcal mol<sup>-1</sup> less stable complex Pd(η<sup>2</sup>-*endo*-NBD)(AF) (**9**).

The step of oxidative addition of AF for complexes **5**, **8**, and **9** (Scheme 3) occurs with a decrease in  $\Delta G_{298}$  in all cases. The products of this step are the Pd<sup>II</sup> allyl complexes: Pd(η<sup>3</sup>-C<sub>3</sub>H<sub>5</sub>)(OCHO)(MeCN) (**10**), Pd(η<sup>3</sup>-C<sub>3</sub>H<sub>5</sub>)(OCHO)-(η<sup>2</sup>-*exo*-NBD) (**11**), and Pd(η<sup>3</sup>-C<sub>3</sub>H<sub>5</sub>)(OCHO)(η<sup>2</sup>-*endo*-NBD) (**12**). Complex **12** can readily be rearranged to more stable complex Pd(η<sup>1</sup>-C<sub>3</sub>H<sub>5</sub>)(OCHO)(η<sup>4</sup>-NBD) (**13**) with the bidentate coordination of the NBD ligand. The allyl ligand in complex **13** is coordinated *via* the η<sup>1</sup> mode because of steric hindrances. It was taken into account when modeling the step of oxidative addition of AF that the C–O bond was cleaved through the five-centered TS.<sup>16</sup> The presence of the NBD ligand in complexes **8** and **9** decreases the activation energy of the oxidative addition

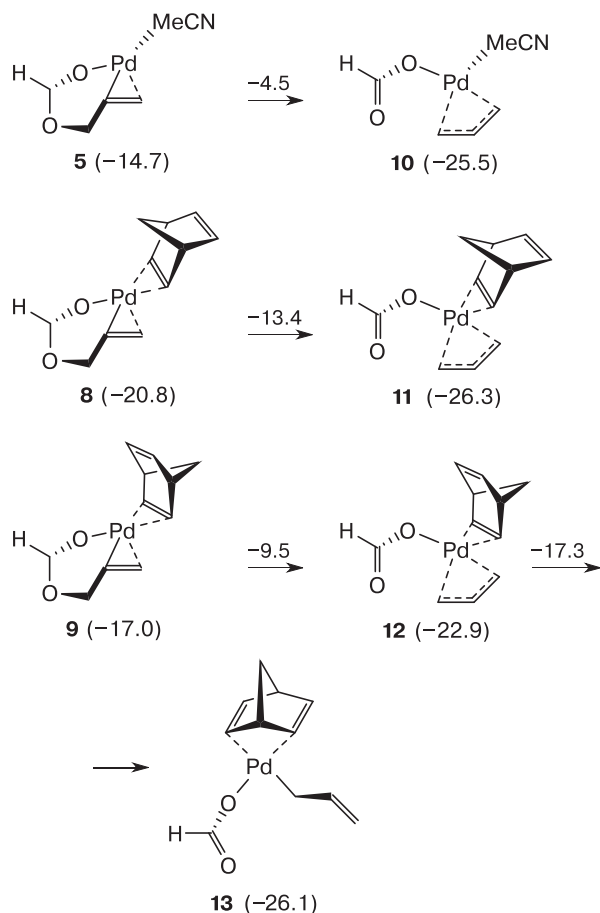
Scheme 2\*



\* Here and further in parentheses, the  $\Delta G_{298}$  values (kcal mol<sup>-1</sup>) are given relative to noninteracting Pd(MeCN)<sub>3</sub> and reactants.

step ( $\Delta\Delta G_{298}^\ddagger = 7.4\text{--}7.5 \text{ kcal mol}^{-1}$ ) compared to the energy determined for step  $5 \rightarrow 10$  ( $\Delta\Delta G_{298}^\ddagger = 10.2 \text{ kcal mol}^{-1}$ ).

Scheme 3\*



\* The  $\Delta G_{298}^\ddagger$  values ( $\text{kcal mol}^{-1}$ ) relative to noninteracting  $\text{Pd}(\text{MeCN})_3$  and reactants are given on arrows in Schemes 3–6.

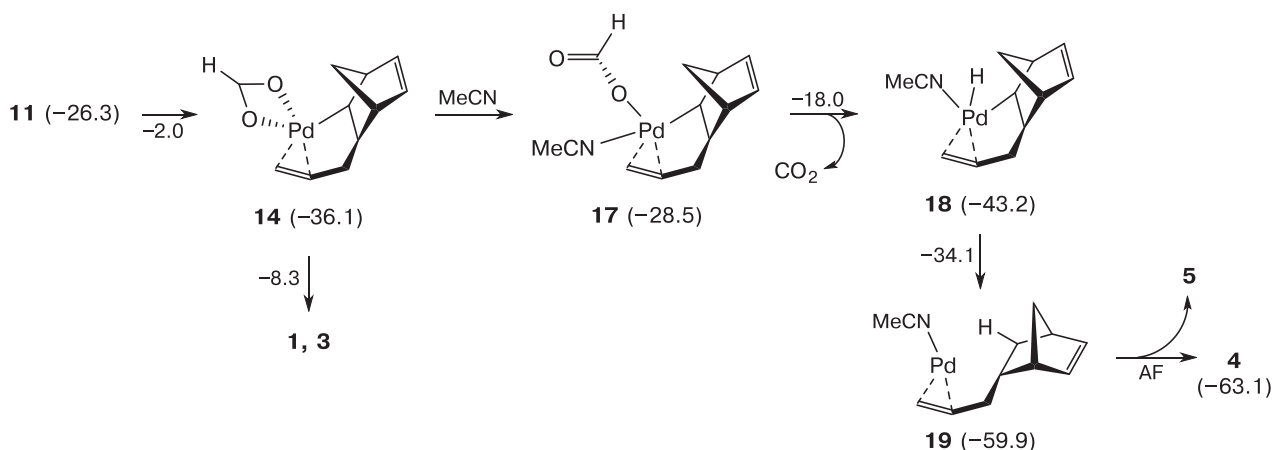
**Mechanism A.** The further development of the hydroallylation mechanism is presented in Scheme 4. The formation of the C–C bond in complexes **11** and **12** gives palladocyclic intermediates **14** and **15** with an appreciable decrease in the energy ( $\sim 10 \text{ kcal mol}^{-1}$ ). The structure of the hydroallylation product is predetermined in this step: *exo*-isomer **4** is formed from complex **11**, whereas *endo*-isomer **4'** is formed from complex **12**. The step is characterized by a high activation barrier of 24.3 and 22.6  $\text{kcal mol}^{-1}$  for transitions  $11 \rightarrow 14$  and  $12 \rightarrow 15$ , respectively. However, the highest activation barrier is observed for step  $13 \rightarrow 16$  ( $\Delta\Delta G_{298}^\ddagger = 40 \text{ kcal mol}^{-1}$ ), indicating that the bond between the  $\eta^4$ -coordinated NBD ligand and  $\eta^1$ -allyl ligand cannot be formed.

The subsequent transformations of intermediate **14** are associated with the turn of the formyl ligand and addition of the solvent molecule to palladium ( $14 \rightarrow 17$ ). The step results in an increase in the Gibbs energy due to a change in the coordination of the formyl ligand by the energetically less favorable coordination mode. However, this rearrangement is important for the subsequent step of hydride transfer from the formyl ligand to the Pd atom ( $17 \rightarrow 18$ ) and is over-compensated by the exothermic elimination of  $\text{CO}_2$  and formation of hydride complex **18**. The backward hydride transfer from the Pd atom to the NBD fragment ( $18 \rightarrow 19$ ) also occurs with an exothermic effect. In the last step ( $19 \rightarrow 5$ ), the formed product **4** is substituted by the AF molecule to form complex  $\text{Pd}(\text{AF})(\text{MeCN})$  (**5**), which returns to a new catalytic cycle.

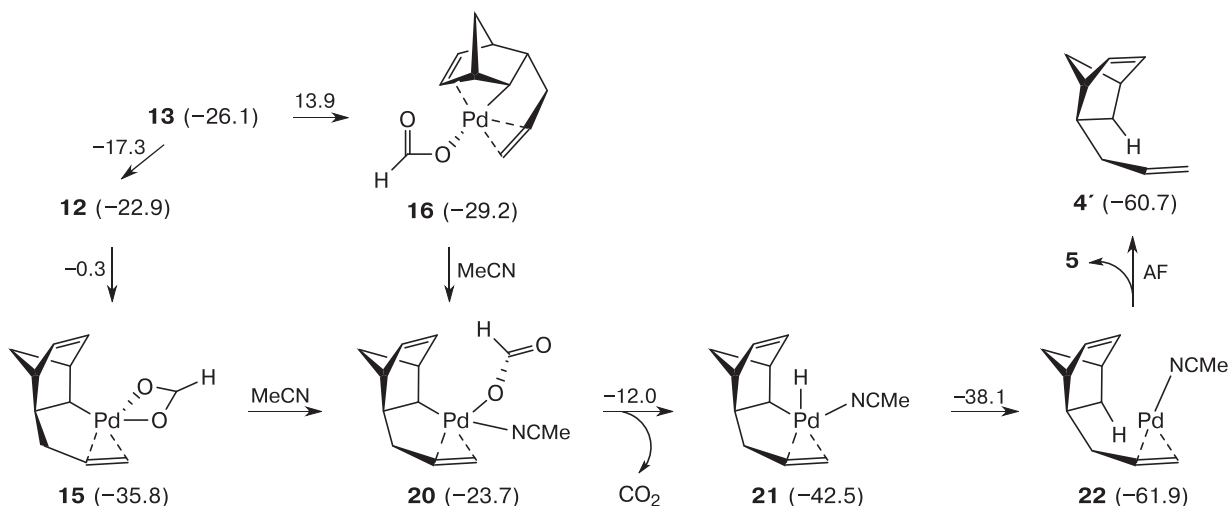
The formation in intermediate **14** of the second C–C bond necessary for the oxidative addition products **1** and **3** seems to be hardly possible because of the high energy barrier ( $\Delta\Delta G_{298}^\ddagger = 27.8 \text{ kcal mol}^{-1}$ ). This makes it possible to explain the predominant formation of the reductive allylation product (**4**) in the absence<sup>6</sup> of phosphine ligands.

*endo*-Isomer **4'** is formed similarly in transitions  $15 \rightarrow 20 \rightarrow 21 \rightarrow 22 \rightarrow 5$  (Scheme 5). As for the *exo*-route,

Scheme 4



Scheme 5



the last step affords complex **5**, which can be considered catalytically active.

The energy profile of NBD hydroallylation (Fig. 1) shows that the formation of the C—C bond is characterized by the highest activation barrier. For the route of *exo*-isomer (**4**) formation, the activation Gibbs energy of C—C bond formation (**11** → **14**) is 24.3 kcal mol<sup>-1</sup>. In the route of *endo*-isomer (**4'**) formation, the activation barrier for C—C bond formation (**12** → **15**) is 22.6 kcal mol<sup>-1</sup>. However, with allowance for the possibility of isomerization of complex Pd( $\eta^2$ -*endo*-NBD)( $\eta^3$ -C<sub>3</sub>H<sub>5</sub>)(OCHO) (**12**) to thermodynamically more stable Pd( $\eta^4$ -NBD)( $\eta^1$ -C<sub>3</sub>H<sub>5</sub>)(OCHO) (**13**), the activation Gibbs energy for the formation of isomer **4'** would correspond to the difference in energies of complex **13** and TS (**12** → **15**), *i.e.*, 25.8 kcal mol<sup>-1</sup>. In this case, the  $\Delta G_{298}^\ddagger$  value is

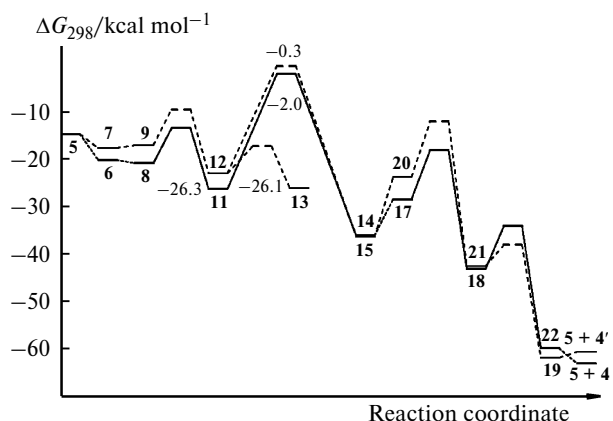


**Fig. 1.** Energy profile of NBD hydroallylation *via* mechanism A. Solid line corresponds to the route for the formation of the *exo*-isomer of 5-allyl-2-norbornene (**4**), and dashed line indicates the route for the formation of the *endo*-isomer of 5-allyl-2-norbornene (**4'**).

1.5 kcal mol<sup>-1</sup> higher than the energy found for the route of formation of complex **4**. In addition, in the hydride transfer step (**17** → **18** and **20** → **21**), the difference in the activation barriers increases to 6 kcal mol<sup>-1</sup>. These two kinetic factors result in the formation of the *exo*-product of NBD hydroallylation only, which is consistent with experimental<sup>9</sup> data.

**Mechanism B.** The KIE of NBD hydroallylation with a value of 2.2, was earlier<sup>9</sup> determined using C<sub>3</sub>H<sub>5</sub>COOD on the deuterium distribution in the products of NBD hydroallylation. This fact indicates that the hydride transfer from the formyl ligand to the Pd atom should occur at the rate-determining step. Our calculations showed that the reaction mechanism is possible where the hydride transfer precedes the step of C—C bond cleavage.

Mechanism B for the formation of product **4** initiated by the turn of the formyl ligand in intermediate **11** and containing the step of the subsequent cleavage of the C—H bond (**11** → **23** → **24**) is presented in Scheme 6. As a result, hydride intermediate **24** is formed capable of transforming *via* the following route: the C—C bond is formed first (**24** → **25**), then the MeCN molecule is added (**25** → **18**) followed by the hydride transfer from the Pd atom to the NBD fragment occurs (**18** → **19**), and, finally, product **4** eliminates.

Another pathway of mechanism B is of interest because it is associated with the formation of intermediate **26** including the agostic interaction. The very high activation barrier ( $\Delta\Delta G_{298}^\ddagger = 37.3$  kcal mol<sup>-1</sup>) should be surmounted to form the C—C bond in complex **26**, since coordinatively unsaturated complex **27** is formed. The activation barrier for the formation of the C—C bond is appreciably lower if the MeCN (**26** → **28** → **19**) or AF (**26** → **29** → **30**) molecule is preliminarily coordinated.

As can be seen from the profile of the Gibbs energy of the reaction (Fig. 2), the first pathway of mechanism B

Scheme 6

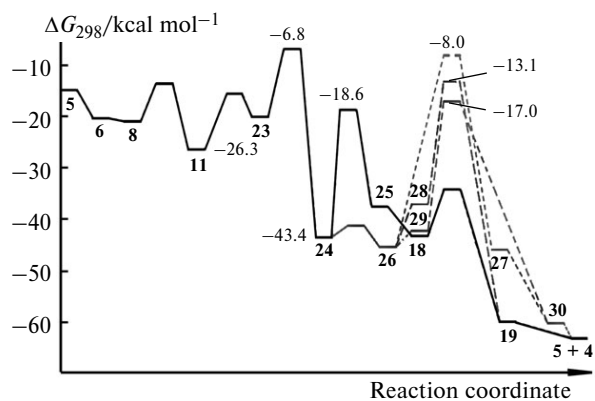
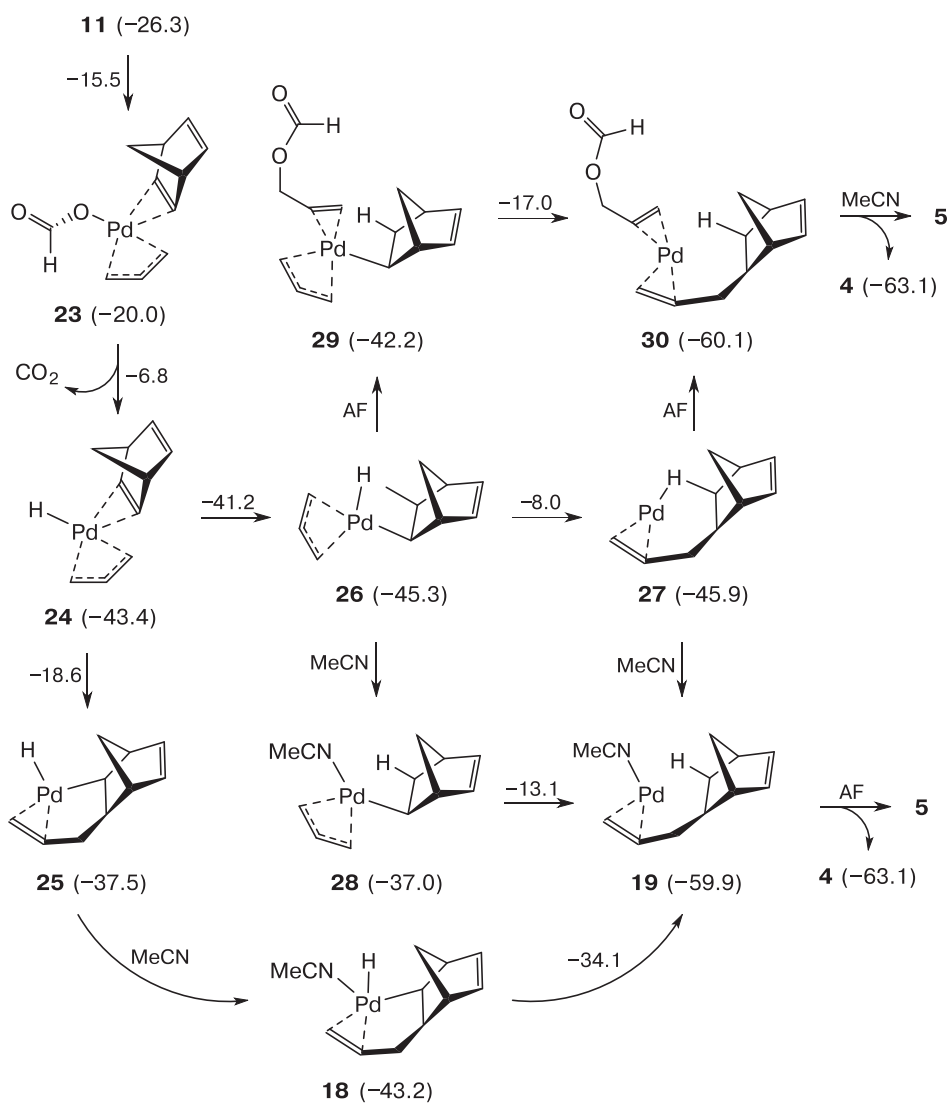


**Fig. 2.** Energy profile of NBD hydroallylation *via* mechanism *B*. Solid line corresponds to the most probable route for the formation of 5-allyl-2-norbornene (**4**), and dashed lines correspond to routes **26**  $\rightarrow$  **27**  $\rightarrow$  **30**, **26**  $\rightarrow$  **28**  $\rightarrow$  **19**, and **26**  $\rightarrow$  **29**  $\rightarrow$  **30**.

(**11**  $\rightarrow$  **23**  $\rightarrow$  **24**  $\rightarrow$  **25**  $\rightarrow$  **18**  $\rightarrow$  **19**  $\rightarrow$  **5**) is preferable from the kinetic point of view since it is associated with the need to cross a lower activation barrier. As in the case of mechanism *A*, the step of C–C bond formation has the highest activation barrier in the reaction route *via* mechanism *B*. If ignoring solvation, the activation Gibbs energy ( $\Delta G^\ddagger_{298}$ ) is 24.3 and 24.8 kcal mol $^{-1}$  for steps **11**  $\rightarrow$  **14** and **24**  $\rightarrow$  **25**, respectively. With allowance for the solvation energy calculated in the IPCM approximation, the values ( $\Delta G^\ddagger_{298, \text{IPCM}}$ ) decrease to 22.7 and 23.3 kcal mol $^{-1}$ , respectively. The additional introduction of two MeCN molecules into the modeling of steps **11**  $\rightarrow$  **14** and **24**  $\rightarrow$  **25** (Fig. 3) and allowance for the solvation energy in the IPCM result in a change in  $\Delta G^\ddagger_{298, 2+ \text{IPCM}}$  to 22.8 and 21.3 kcal mol $^{-1}$ , respectively.

Now we can consider calculations taking into account two mechanisms that mainly differ by the order of occur-

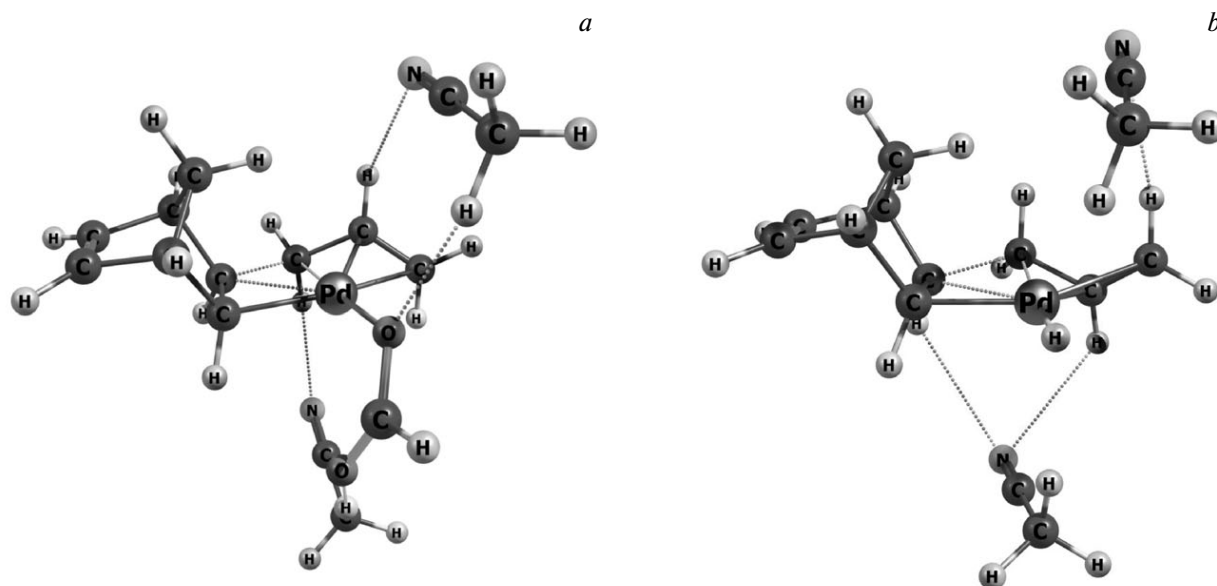


Fig. 3. Optimized structures of TS for steps **11** → **14** (a) and **24** → **25** (b), which are solvated by two acetonitrile molecules.

rence of steps of C—C bond formation and hydride transfer from the formyl ligand. The results show that the rate of cleavage of the C—H bond in steps **17** → **18** and **23** → **24** cannot determine the hydroallylation rate. As could be expected, the theoretical calculation of the  $k_{\text{H}}/k_{\text{D}}$  ratio for the steps of C—C bond formation (**11** → **14** and **24** → **25**) results in the absence of the KIE (Table 1). Assuming that the hydride transfer with the C—H bond cleavage is the rate-determining step in NBD hydroallylation, the theoretical value is  $k_{\text{H}}/k_{\text{D}} \approx 4.7$  (see Table 1). This value is more than twice as large as the experimental estimate<sup>9</sup> for the KIE of NBD hydroallylation.

Although the activation barrier for the hydride transfer **23** → **24** in mechanism *B* is lower than that for the C—C bond formation, the hydride transfer step is irreversible, since the activation energy of the direct transformation of hydride intermediate **24** (**24** → **25**) is considerably lower than the activation energy of the backward process (**24** → **23**). Therefore, the hydride transfer affects the selectivity of the reaction. Similarly, in mechanism *A* the hydride transfer step **17** → **18** is irreversible. The theoretical analysis<sup>17,18</sup> shows that both the rate constant of the rate-determining step and the rate constant of the

irreversible step before or after the rate-determining step can affect the KIE value of the catalytic reaction, since the irreversible step determines the selectivity of the isotope distribution in the products. Therefore, we may conclude that product **4** is formed in parallel *via* two considered mechanisms with close activation energies. The observed KIE value equal to 2.2 is intermediate and determined by the rate constants of the rate-determining step of C—C bond formation and irreversible step of hydride transfer in these mechanisms.

Thus, the results of quantum chemical modeling of the reductive allylation of NBD supplement and refine the concepts about the reactions of NBD with AF in the presence of the Pd<sup>0</sup> acetonitrile complexes. An analysis of the energy profiles assumes that 5-allyl-2-norbornene is formed *via* two mechanisms. In the first of them, the C—C bond between the NBD and allyl ligand is formed before the step of formyl C—H bond cleavage (and before elimination of CO<sub>2</sub>), while in the second case the bond is formed after these processes. In both cases, complex Pd(AF)(MeCN) is catalytically active and the C<sub>NBD</sub>—C<sub>All</sub> bond is formed in the rate-determining step with the Gibbs activation energy equal to 22.8 and 21.3 kcal mol<sup>-1</sup> for the first and second mechanism, respectively.

A high selectivity to 5-allyl-2-norbornene is attributable to the kinetically hindered formation of the second C—C bond needed for the generation of oxidative allylation products. The predominant formation of the *exo*-substituted product is related to the formation of the thermodynamically stable complex with the bidentate coordination of the NBD molecule during its *endo*-coordination.

Further theoretical studies of oxidative allylation in the presence of the Pd<sup>0</sup> complexes and the influence of

Table 1. Results of the calculation of the KIE for various steps of NBD hydroallylation

Step	Reaction	$k_{\text{H}}/k_{\text{D}}$
Formation of C—C bond	<b>11</b> → <b>14</b>	1.02
	<b>24</b> → <b>25</b>	1.01
Cleavage of C—H bond	<b>17</b> → <b>18</b>	4.67
	<b>23</b> → <b>24</b>	4.72

the phosphine ligands on the reaction mechanism are desirable to present the full pattern of the mechanism for the reactions of NBD with allyl carboxylates.

This work was financially supported by the Russian Science Foundation (Project No. 18-13-00415). The calculations were performed using computational resources of the Joint Supercomputer Center of the Russian Academy of Sciences.

### References

1. V. R. Flid, M. L. Gringolts, R. S. Shamsiev, E. Sh. Finkelshtein, *Russ. Chem. Rev.*, 2018, **87**, 1169.
2. M. Catellani, G. Chiusoli, E. Dradi, G. Salerno, *J. Organomet. Chem.*, 1979, **177**, 29.
3. U. M. Dzhemilev, R. I. Khusnutdinov, G. A. Tolstikov, *Russ. Chem. Rev.*, 1987, **56**, 36.
4. U. M. Dzhemilev, R. I. Khusnutdinov, D. K. Galeev, O. M. Nefedov, G. A. Tolstikov, *Bull. Acad. Sci. USSR, Div. Chem. Sci.*, 1987, **36**, 122.
5. E. M. Evstigneeva, R. S. Shamsiev, V. R. Flid, *Vestn. MITKhT im. M. V. Lomonosova [Bulletin of M. V. Lomonosov Moscow Institute of Chemical Technologies]*, 2006, **1**, No. 3, 3 (in Russian).
6. E. M. Evstigneeva, V. R. Flid, *Russ. Chem. Bull.*, 2008, **57**, 837.
7. I. P. Stolyarov, A. E. Gekhman, I. I. Moiseev, A. Yu. Kolesnikov, E. M. Evstigneeva, V. R. Flid, *Russ. Chem. Bull.*, 2007, **56**, 320.
8. S. A. Durakov, R. S. Shamsiev, V. R. Flid, A. E. Gekhman, *Russ. Chem. Bull.*, 2018, **67**, 2234.
9. S. A. Durakov, R. S. Shamsiev, V. R. Flid, A. E. Gekhman, *Kinet. Catal.*, 2019, **60**, 245.
10. D. N. Laikov, *Chem. Phys. Lett.*, 1997, **281**, 151.
11. D. N. Laikov, Yu. A. Ustynuk, *Russ. Chem. Bull.*, 2005, **54**, 820.
12. J. P. Perdew, K. Burke, M. Ernzerhof, *Phys. Rev. Lett.*, 1996, **77**, 3865.
13. D. N. Laikov, *Chem. Phys. Lett.*, 2005, **416**, 116.
14. R. S. Shamsiev, V. R. Flid, *Russ. Chem. Bull.*, 2013, **62**, 2301.
15. D. V. Dmitriev, R. S. Shamsiev, Ha Ngok Thien, V. R. Flid, *Russ. Chem. Bull.*, 2013, **62**, 2385.
16. K. T. Egiazaryan, R. S. Shamsiev, V. R. Flid, *Fine Chem. Technol.*, 2019, **14**, No. 6, 56.
17. E. M. Simmons, J. F. Hartwig, *Angew. Chem., Int. Ed.*, 2012, **51**, 3066.
18. Z. Mao, C. T. Campbell, *ACS Catal.*, 2020, **10**, 4181.

Received August 25, 2020;  
in revised form October 20, 2020;  
accepted November 2, 2020